

**PROJECT FOR RESEARCH AND DEVELOPMENT OF DEMINING  
RELATED EQUIPMENT IN CAMBODIA**

**No 3**

**SURVIVABILITY TEST**

**SWING TYPE MACHINE**

## 8. INTRODUCTION

This measurement test intends to evaluate the safety of cabin crews in demining machines. The sound pressure and vibration/acceleration in the machine cabin at mine blast will be measured in this experimental study. Sound overpressure can damage the ears of the machine operator and excess vibration and acceleration can cause injuries to his/her foot, ankle and spine. We follow the test procedures and safety criteria defined in the FMV Swedish Defense Material Administration document 1). This paper reports on-site test results in Cambodia, analyses the measurement data collected, and examines the safety of demining machines.

## 9. TEST METHOD

### 9.1. DEMINING MACHINES UNDER TEST

Demining Machine #1: Made by YAMANASHI HITACHI, Swing-type (Referred as YAMANASHI S)

### 9.2. MEASUREMENT SYSTEM CONFIGURATION

The configuration of the measurement system is shown in figure below. The sound pressure and vibration/ acceleration in the cabin of demining machines are measured in the following locations:

- Sound Pressure: Place a pair of pressure sensors and a probe of sound-level meter about the height of the operator's ear,
- Vibration/Acceleration: Set one accelerometer on the cabin floor and another on the top of the weight of 60kg placed on the operator seat to emulate a human weight. The blast pressure at the flail will be measured for Machine #1 (YAMANASHI S).

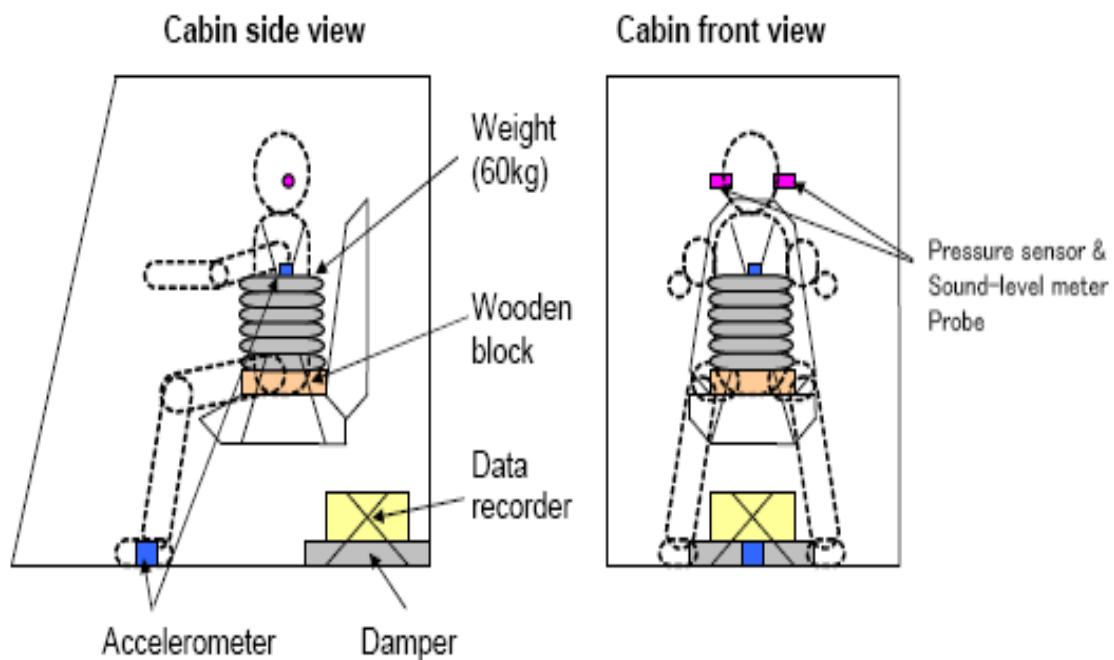


Figure 82: Measurement System Configuration

### 9.3. TEST EQUIPMENT

- Sound-Level Meter: NA-42 (RION)
- Pressure Sensor: PHL-A-1MP (KYOWA) , Full-Scale 200 kPa
- Accelerometer: AS-100HA (KYOWA), Full Scale 100G
- A data recorder is placed in the demining machine cabin and the measurement data with the equipment listed above are logged. The sampling rate is set no lower than 20 kHz.
- Data Recorder: EDX-2000A-32 (KYOWA)

- Maximum number of data channels: 32ch, A/D Resolution: 16 bit
- Maximum Sampling Rate: 200 kHz
- Bandwidth: DC to 50 kHz (Pressure Sensor Amplifier)
- DC to 20 kHz (Accelerometer Amplifier)

#### 9.4. EXPLOSIVES USED

The explosives listed below are used in the experiments.

- Anti-personnel Mine: C4 equivalent to TNT 100g
- Anti-tank Mine: A combination of a mine (equivalent to TNT 6kg) & C4 (equivalent to 2kg)
- CMAC (Cambodian Mine Action Center) mine specialists are responsible for all the explosive handling



Figure 83: a combination of Anti-tank and C4 to be exploded  
Under the attachment

#### 10. ON-SITE TEST

##### 10.1. TEST SITE

(The same place with test No.1)

- Province: Siem Reap province
- District: Sort Nikum
- Commune: Porpel
- Village: Porpel kandaal

##### 10.2. TEST PREPARATION

The machine is placed 300m from the command and control point (also house a visitors). Surrounding the machine is high pile of earth protected by sand bags. All the arrangement and preparation is made according to CMAC safety standard operating procedure.



Figure 84: Survivability test spot of the machine

### 10.3. TEST SCHEDULE

Table 54: Test Schedule

Date	Place	Mission
Aug. 25, 2006	-	Transportation (Leave from Tokyo)
Aug. 26, 2006	CMAC Test Site (Siem Reap Vicinity)	Unpacking and preparing for tests
Aug. 28, 2006	CMAC Test Site (Siem Reap Vicinity)	Anti-personnel Mine Test
Aug. 29, 2006	CMAC Test Site (Siem Reap Vicinity)	Anti-tank Mine Test
Aug. 30, 2006	CMAC Test Site (Siem Reap Vicinity)	Test site cleaning, equipment packing and staff meeting
Aug. 31, 2006	Hotel (Siem Reap)	Data validity check
Sept. 1, 2006	Hotel (Siem Reap)	Data review, Packing
Sept. 2, 2006	-	Transportation
Sept. 3, 2006	-	Transportation (Arrive in Tokyo)

### 10.4. MEASUREMENT WORK DETAILS

Table 55: Measurement Work Details

Date	Work Details
Aug. 28, 2006	Installed cables Anti-personnel mine test - Installed equipment - Checked sensor signals - Collected data at an anti-tank mine blast - Checked quickly measured data
Aug. 29, 2006	Anti-tank mine test on - Checked sensor signals - Collected data at an anti-tank mine blast - Checked quickly measured data - Uninstalled equipment - Uninstalled cables

## 11. EXPERIMENTAL RESULTS

### 11.1. MEASUREMENT SYSTEM INSTALLATION

The views of measurement system installed in the test machine cabins are shown in Figures 2 to 9. The pressure sensors, the sound-level meter and its probe, and data recorder are strapped down to the cabin interiors. The weight made of 6 pieces of 10kg iron disk and the wooden block are also bound to the operator seat with strings. The accelerometers are glued to the cabin floor and seat weight surfaces.



Figure 85: Equipment Installation in the Machine [1/4]



Figure 86: Equipment Installation in the Machine [2/4]



Figure 87: Equipment Installation in the Machine [3/4]



Figure 88: Equipment Installation in the Machine [4/4]

## 11.2. TEST RESULTS

### 11.2.1. SOUND PRESSURE

- Measured sound pressures in the machine cabin for anti-personnel landmine are shown in figures below:

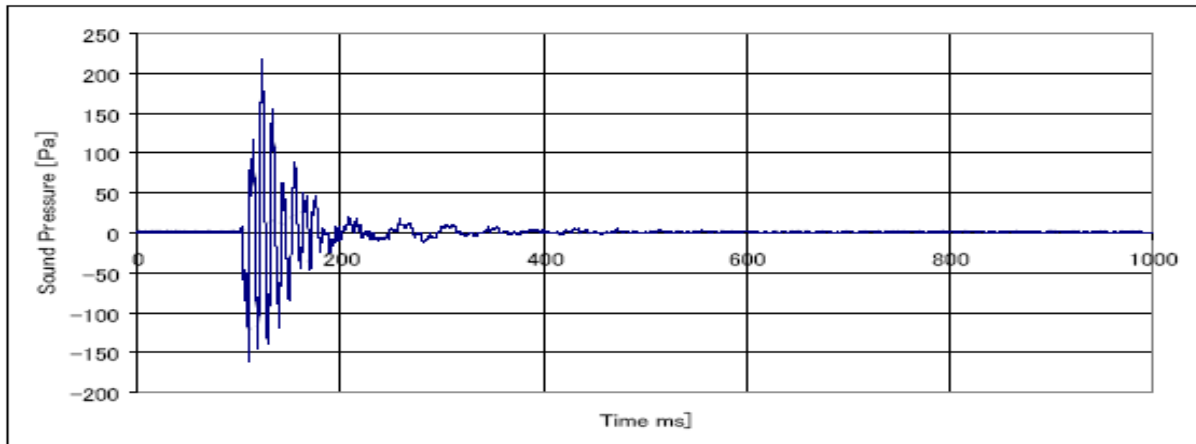


Figure 89: Sound Pressure in the Yamanashi swing type machine - Anti-personnel landmine [1/2]

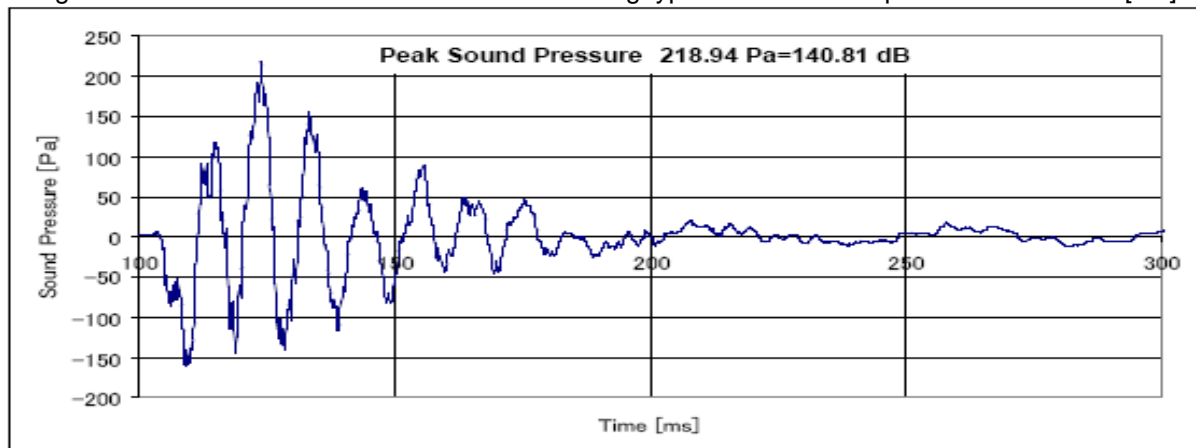


Figure 90: Sound Pressure in the Yamanashi swing type machine - Anti-personnel landmine [2/2]

- Measured sound pressures in the machine cabin for anti-tank mine are shown below:

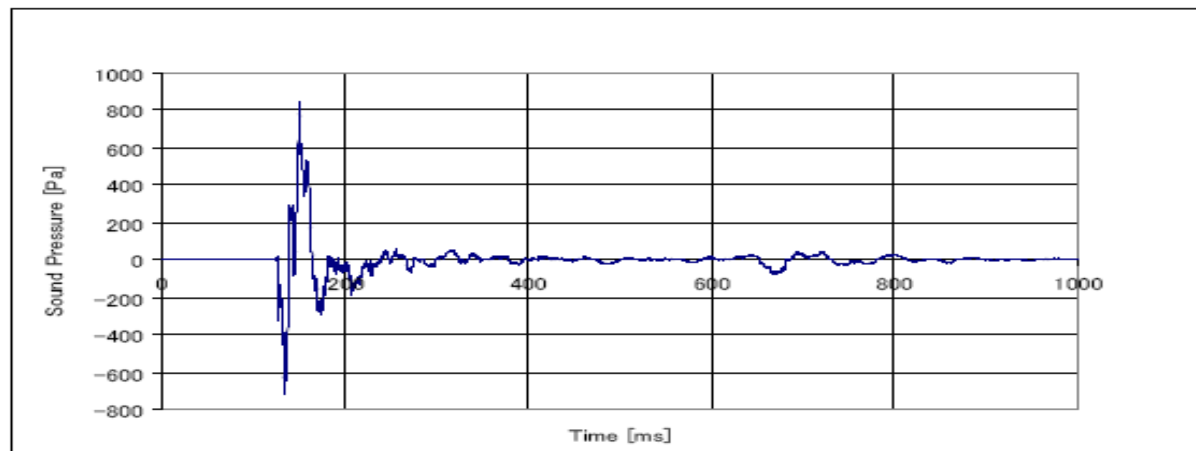


Figure 91: Sound Pressure in the Yamanashi swing type machine - Anti-tank mine [1/2]

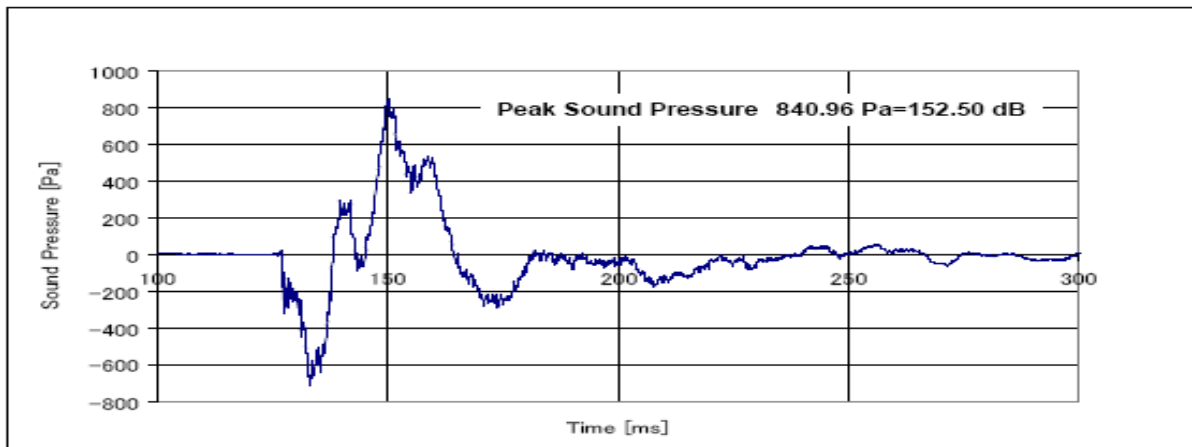


Figure 92: Sound Pressure in the Yamanashi swing type machine - Anti-tank mine [2/2]

**11.2.2. CABIN PRESSURE CHANGE**

- Measured cabin pressure changes resulted from anti-personnel mine are shown in figure below:

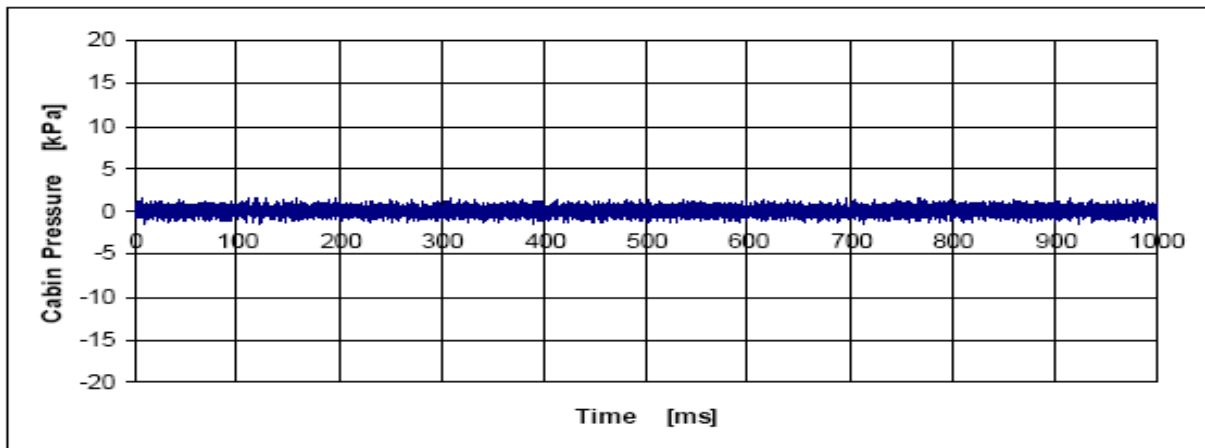


Figure 93: Cabin Pressure in the Yamanashi swing type machine - Anti-personnel Mine

- Measured cabin pressure changes resulted from anti-tank mine are shown in figure below:

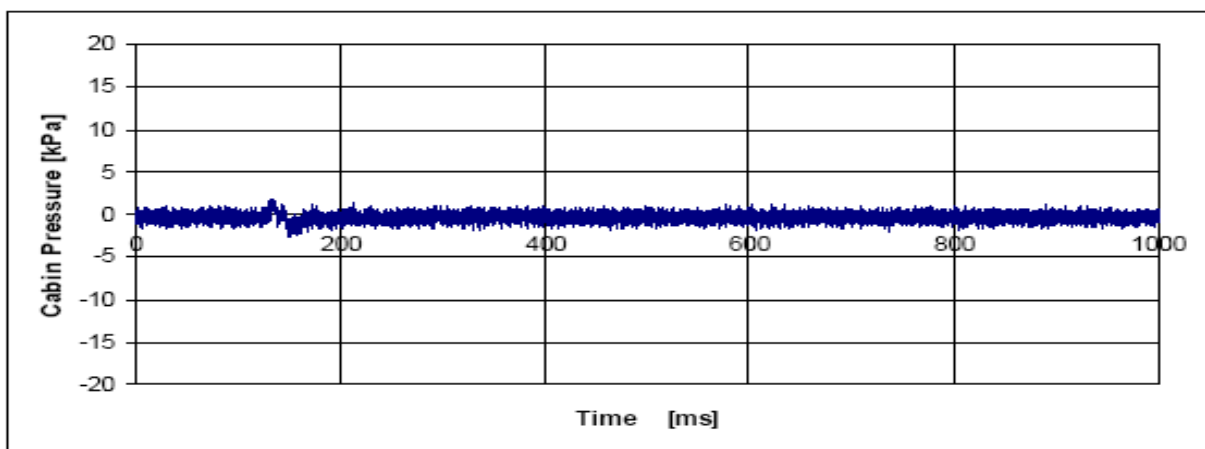


Figure 94: Cabin Pressure in the Yamanashi swing type machine - Anti-tank Mine

### 11.2.3. FLOOR ACCELERATION

- Acceleration data resulted from the Anti-personnel mine are shown in figures below:

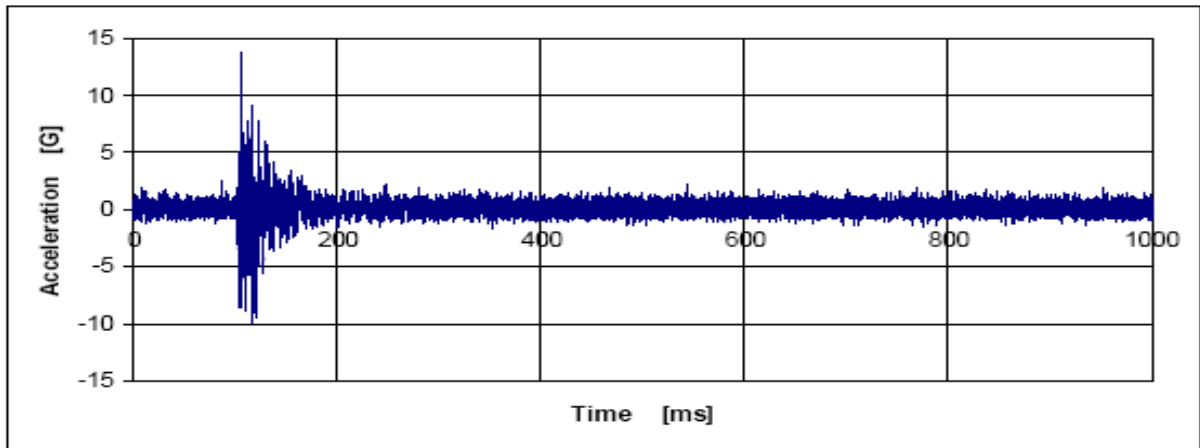


Figure 95: Floor Acceleration in Yamanashi Hitachi swing type- Anti-personnel Mine [1/2]

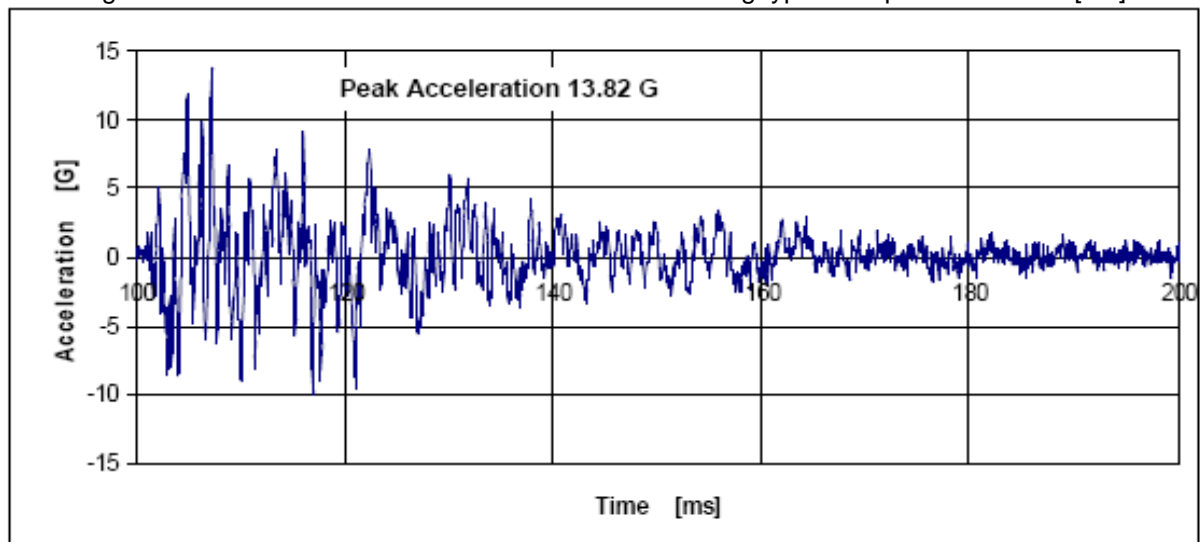


Figure 96: Floor Acceleration in Yamanashi Hitachi swing type- Anti-personnel Mine [2/2]

- Acceleration data resulted from the Anti-tank mine are shown in figures below:

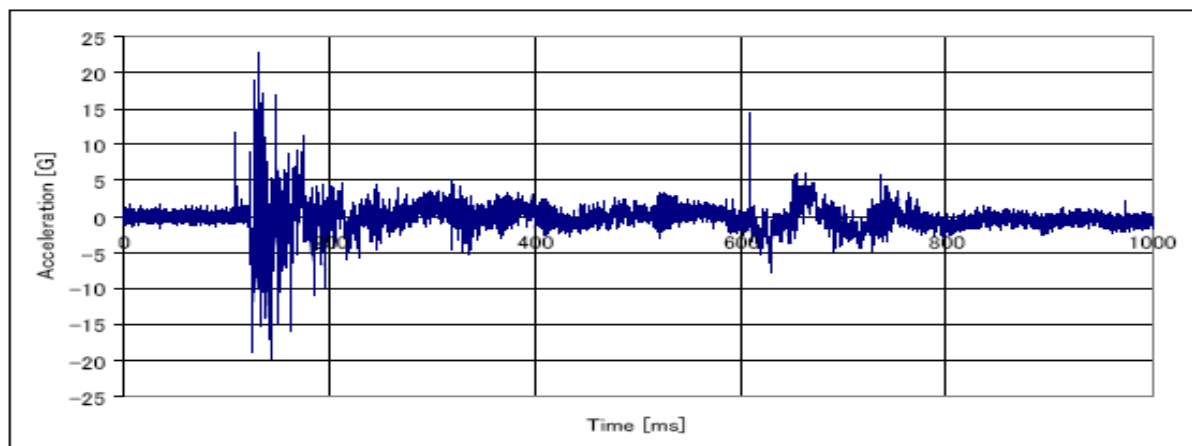


Figure 97: Floor Acceleration in Yamanashi Hitachi swing type- Anti-tank Mine [1/2]



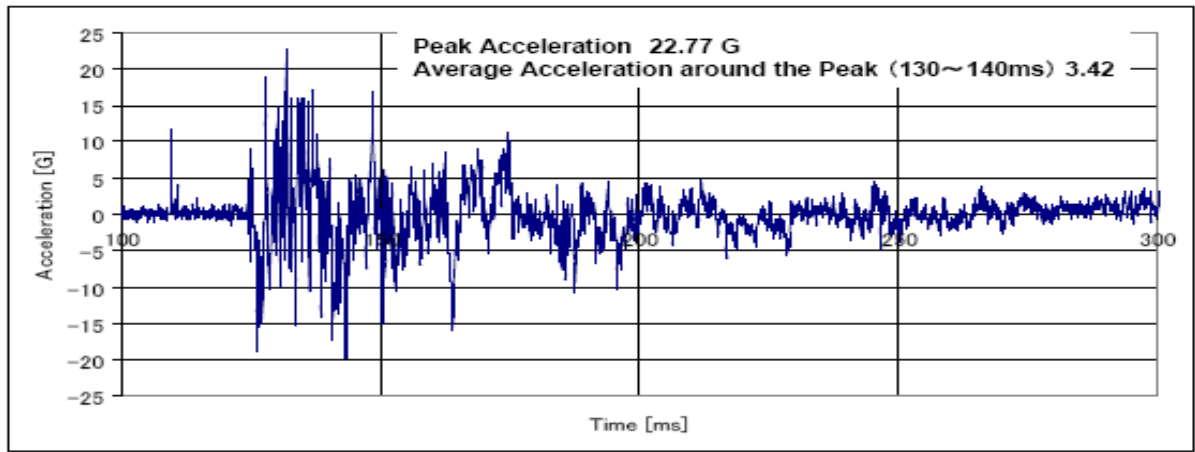


Figure 98: Floor Acceleration in Yamanashi Hitachi swing type- Anti-tank Mine [2/2]

**11.2.4. SEAT ACCELERATION**

- Acceleration data resulted from the Anti-personnel mine are shown in figures below:

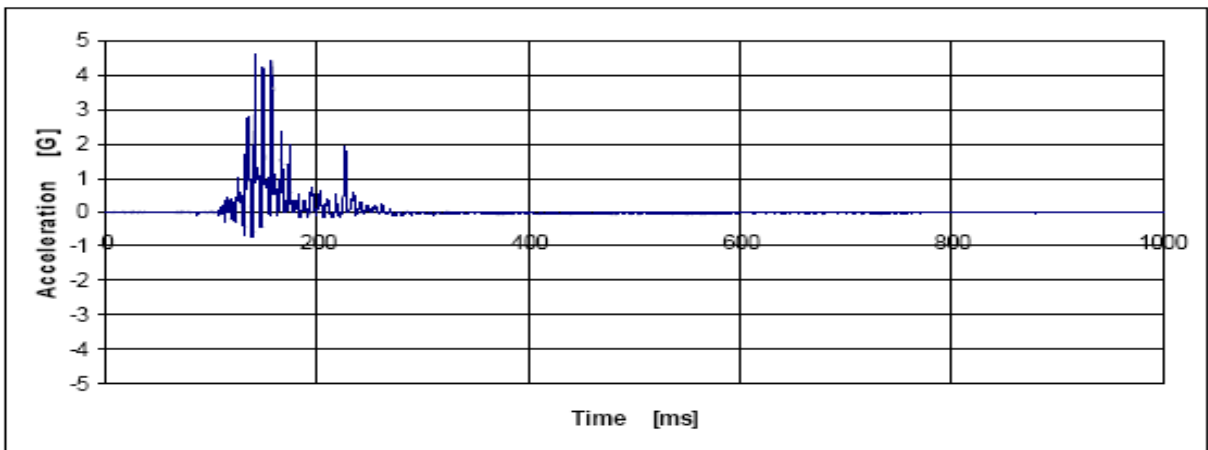


Figure 99: Seat Acceleration in Yamanashi Hitachi swing type- Anti-Personnel Mine [1/2]

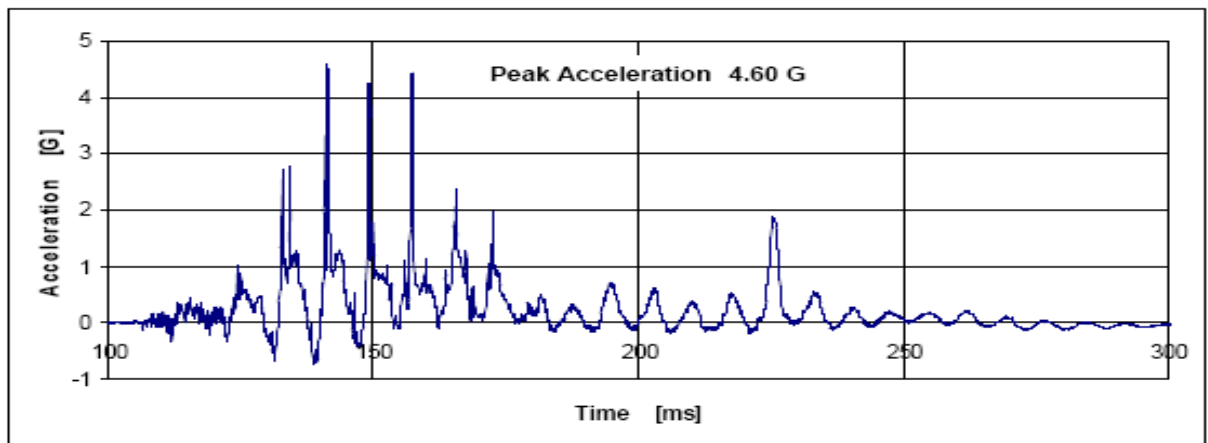


Figure 100: Seat Acceleration in Yamanashi Hitachi swing type- Anti-Personnel Mine [2/2]

- Acceleration data resulted from the Anti-tank mine are shown in figures below:

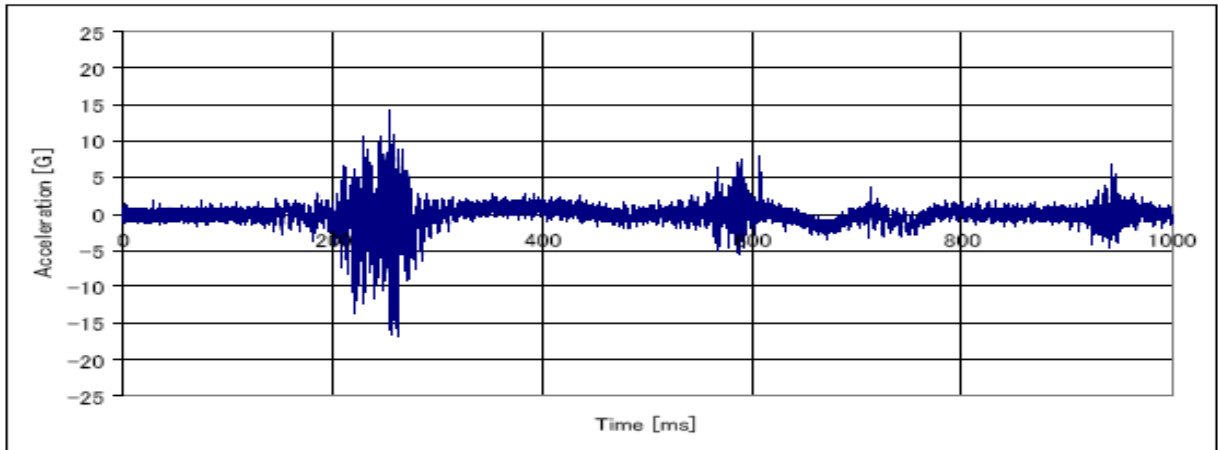


Figure 101: Seat Acceleration in Yamanashi Hitachi swing type- Anti-Tank Mine [1/2]

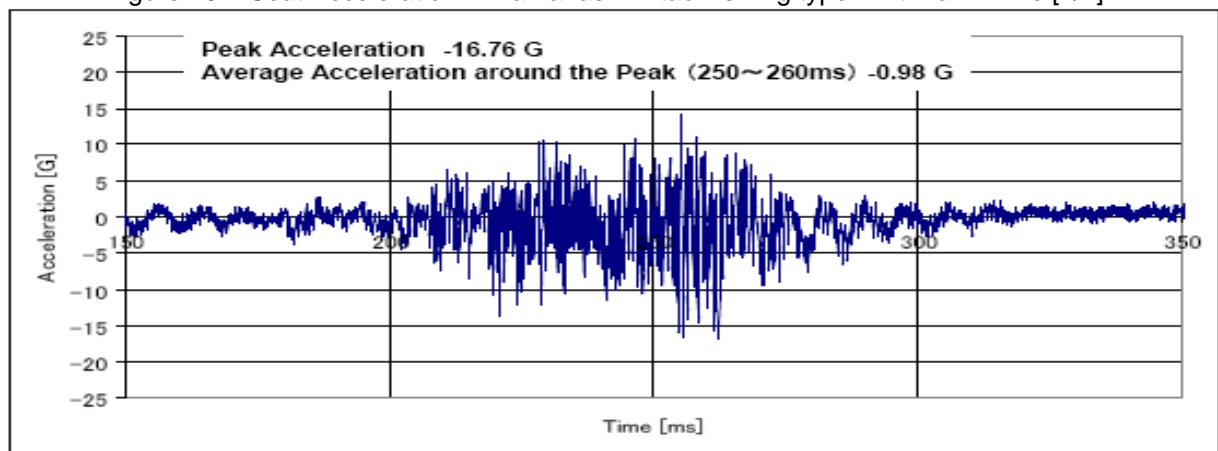


Figure 102: Seat Acceleration in Yamanashi Hitachi swing type- Anti-Tank Mine [2/2]

**11.2.5. BLAST PRESSURE**

- In this experiment the blast pressure was measured in the flail cage with a pressure sensor (installed by YAMANASHI HITACHI). The measurement data of the blast pressure for Anti-personnel mine are shown as follows:

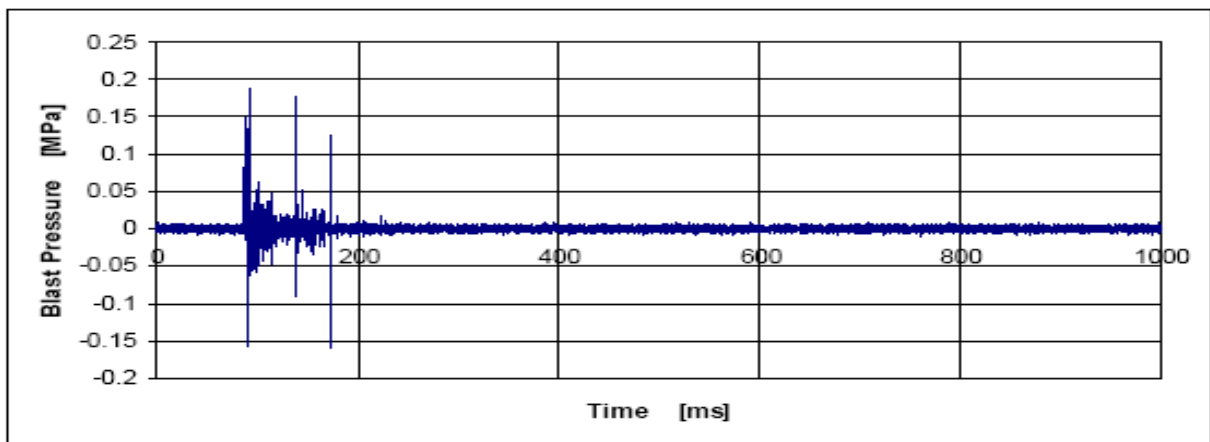


Figure 103: Blast Pressure at in Yamanashi Hitachi swing type - Anti-personnel Mine [1/2]

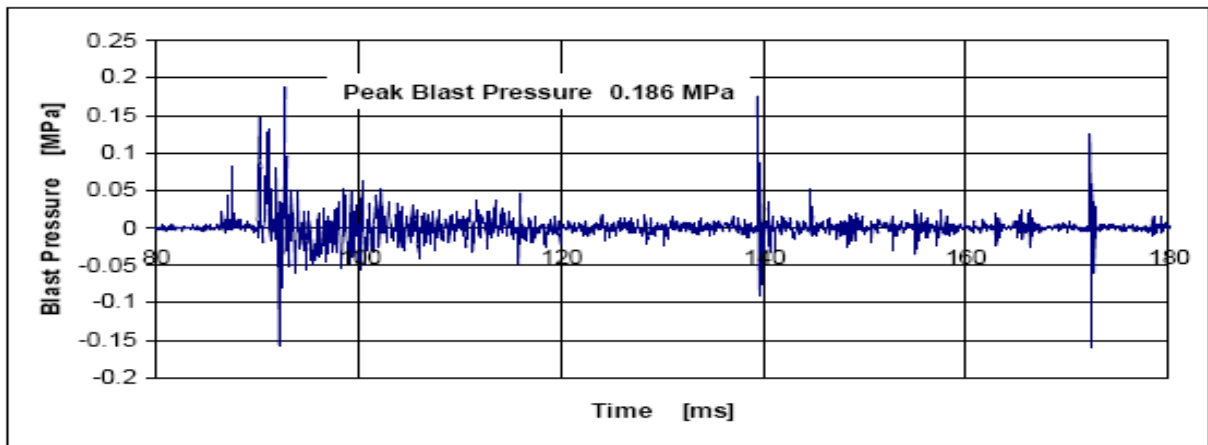


Figure 104: Blast Pressure at in Yamanashi Hitachi swing type - Anti-personnel Mine [2/2]

- The measurement data of the blast pressure for Anti-tank mine are shown as follows:

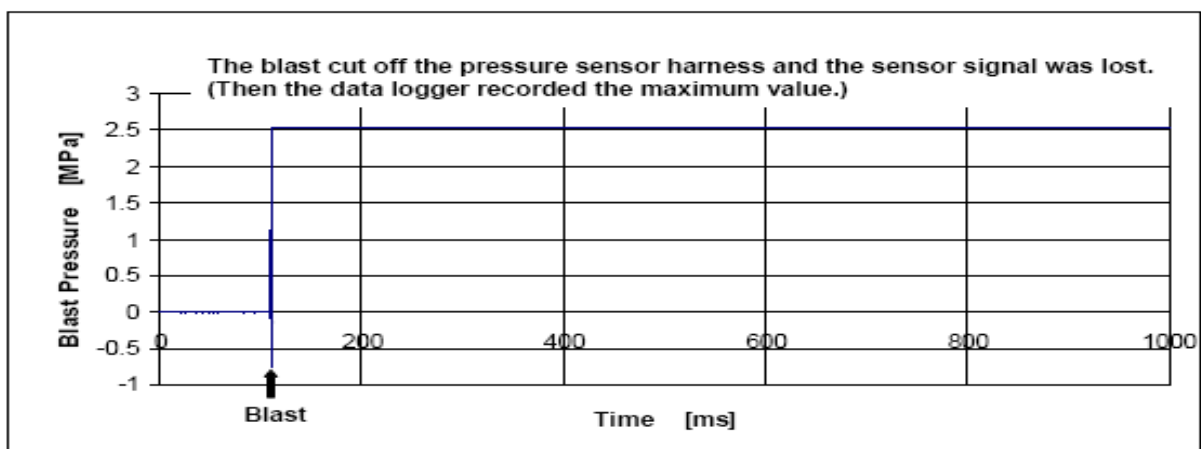


Figure 105: Blast Pressure at in Yamanashi Hitachi swing type - Anti-tank Mine [1/2]

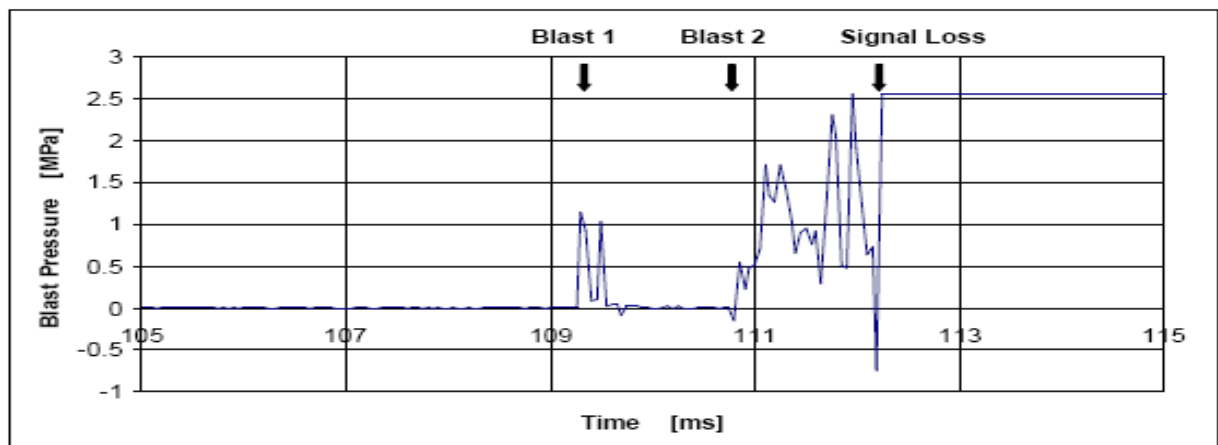


Figure 106: Blast Pressure at in Yamanashi Hitachi swing type - Anti-personnel Mine [2/2]

### 11.3. VERIFYING TEST RESULTS

#### 11.3.1. CABIN PRESSURE CHANGE MEASUREMENT

In this measurement a pair of pressure sensors (with full-scale of 200 kPa) are used assuming poor noise shielding in machine cabins. The sensors measured very little deviation from a noise level at each anti-personnel mine blast. The sensors detected some fluctuation in the cabin pressure at anti-tank mine blast. The pressure data was insignificant and no explosion yielded a pressure change that exceeded 2kPa (≈160dB). The cabin pressure change was found to be no more the 160dB, and therefore, the measurement data with the sound-level meter will be used for the analysis in the following chapters.

### 11.3.2. CORRUPTED DATA

There is no corrupt data in this machine. All the equipment functions well despite strong explosion.

## 12. DATA ANALYSIS

### 12.1. ANALYSIS METHOD

Following the procedures, methods and safety criteria described in the FMV document 1) and MIL Standard 2) we analyze the measured data in order to find if they are in the acceptable level with respect to injuries at ear, foot/ankle and spine. The data analysis methods are discussed below.

### 12.2. EAR INJURY

The peak value of the sound pressure in cabins and B-duration (accumulated duration of excess sound pressure) are extracted from the measurement data.

### 12.3. FOOT AND ANKLE INJURY

The average and maximum of the floor acceleration and maximum velocity change are examined. (See Remark below.)

### 12.4. SPINE INJURY

The average and maximum of the seat acceleration and maximum velocity change are examined. (See Remark below.)

The differential equation (1) is to be analyzed in order to find the DRI (Dynamic Response Index). (See Appendix for the numerical analysis.)

$$\frac{d^2b}{dt^2} + 2\zeta\omega_n \frac{d\delta}{dt} + (\omega_n)^2 \delta = a_c(t) \quad (1)$$

Where:

$\delta$  : Displacement (of a human body modeled as a second order system)

$\zeta$  : Damping coefficient (of the second order system)

$\omega_n$  : Natural angular frequency (of the second order system)

$a_c$  : Applied (=measured) acceleration (to the second order system)

DRI is defined as:

$$DRI = (\omega_n)^2 \delta_{\max} / G \quad (2)$$

Where:

$\delta_{\max}$  : Maximum displacement

$G = 9.8m / s^2$  : Acceleration of Gravity

In DRI calculation, use the values below for the human body model.

$$\zeta = 0.224$$

$$\omega_n = 52.9rad / s (= 8.4Hz)$$

The maximum value of DRI that yields no injury to spines is 16. The equation (2) is rewritten as the equation (3) to find the maximum value of acceptable displacement

$$\delta_{maz} \leq \frac{DRI \times G}{(\omega_n)^2} = \frac{16 \times 9.8m/s^2}{(52.9rad/s)^2} = 56mm \quad (3)$$

Thus, we found the maximum value of the acceptable displacement on the operator seat is 56mm.

## REMARK

The FMV Reports refers to A.E. Hirsch's paper of the dynamic modeling of human body (published in 1967), and details very little about shock motion. We are unable to access the Hirsch paper and have to leave the terminology "max velocity change" unclear. Here we assume the shock motion last fairly short period of time and use 10 ms as its typical duration of the shock. Then, "max velocity change of 3m/s" in 10ms is identical to an average acceleration of 3m/s/10 ms = 300m/s/s = 30.61G. In this report we examine velocity-time charts and look for an abrupt velocity change, i.e., large average acceleration.

## 12.5. DATA ANALYSIS ON YAMANASHI HITACHI SWING TYPE

### 12.5.1. EAR INJURY

- **ANTI-PERSONNEL MINE**

The peak sound pressure in cabin is 218.94 Pa (=140.81 dB) and slightly exceeds the 200 Pa (= 140 dB) limit (see section 11.2.1 for Anti-Personnel mine)

- **ANTI-TANK MINE**

According to figure shown in section 11.2.1 for Anti-tank mine, the peak sound pressure in cabin exceeded 200 Pa. The B-duration of this pressure-time history could be shown as follows:

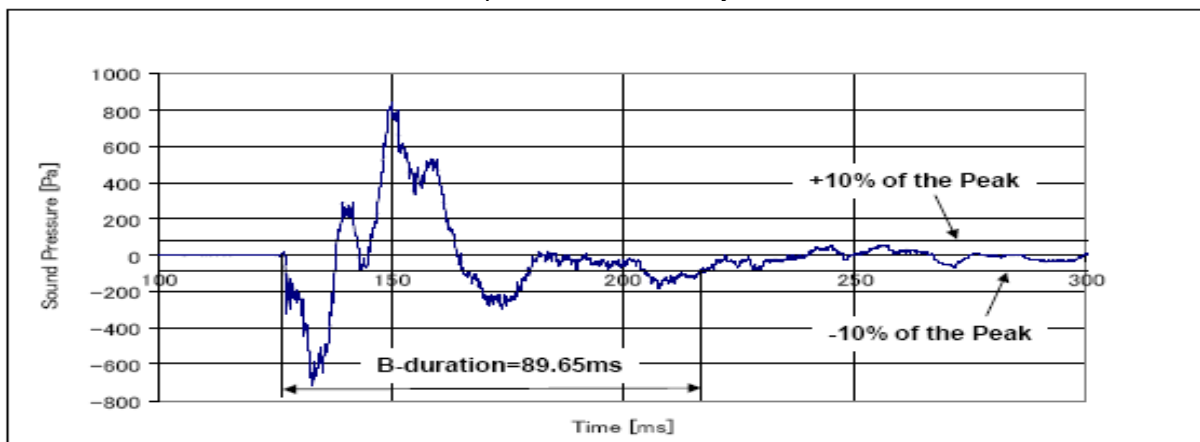


Figure 107: B-duration of Sound Pressure in Yamanashi Hitachi swing type - Anti-tank Mine

### 12.5.2. FOOT AND ANKLE INJURY

- **ANTI-PERSONNEL MINE**

Integration of the floor acceleration by anti-personnel landmine in section 11.2.3 could be shown as follows:

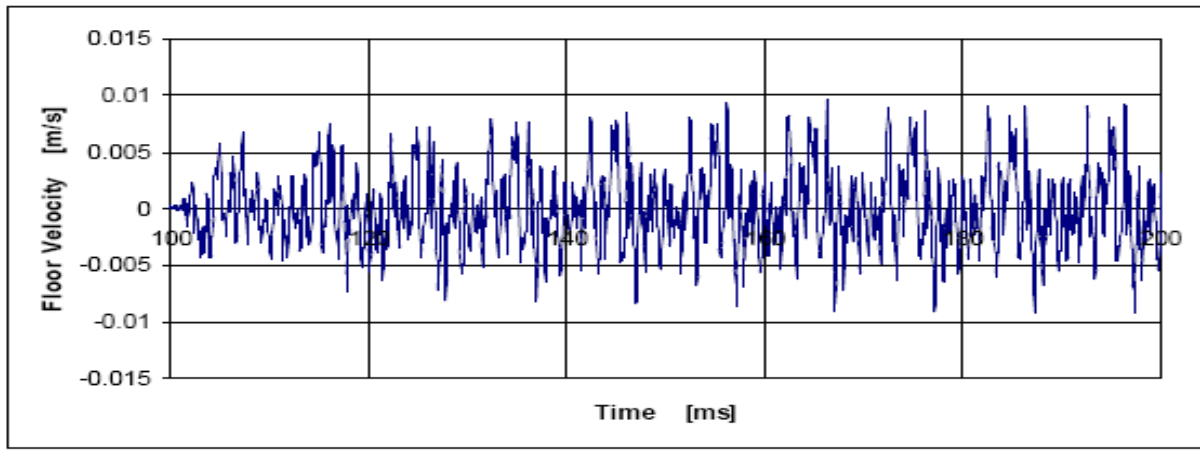


Figure 108: Floor Velocity-Time Chart for Yamanashi Hitachi Swing type - Anti-personnel Mine

- **ANTI-TANK MINE**

Integration of the floor acceleration in the cabin of Yamanashi Hitachi swing type by anti-tank mine blast in section 11.2.3 could be shown as follows:

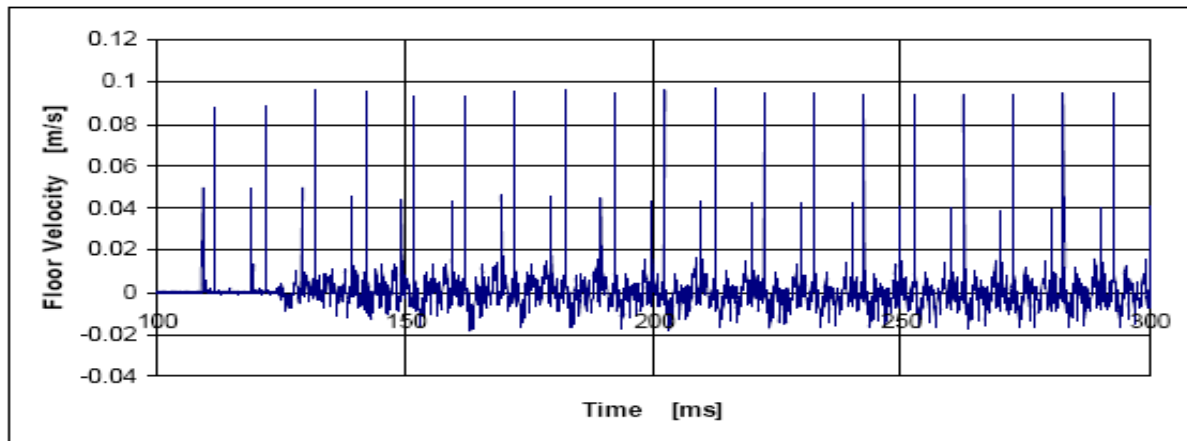


Figure 109: Floor Velocity-Time Chart for Yamanashi Hitachi Swing type - Anti-tank Mine

### 12.5.3. SPINE INJURY

- **ANTI-PERSONNEL MINE**

- Velocity-time chart

Integration of the seat acceleration by Anti – Personnel mine in section 11.2.4 is shown below:

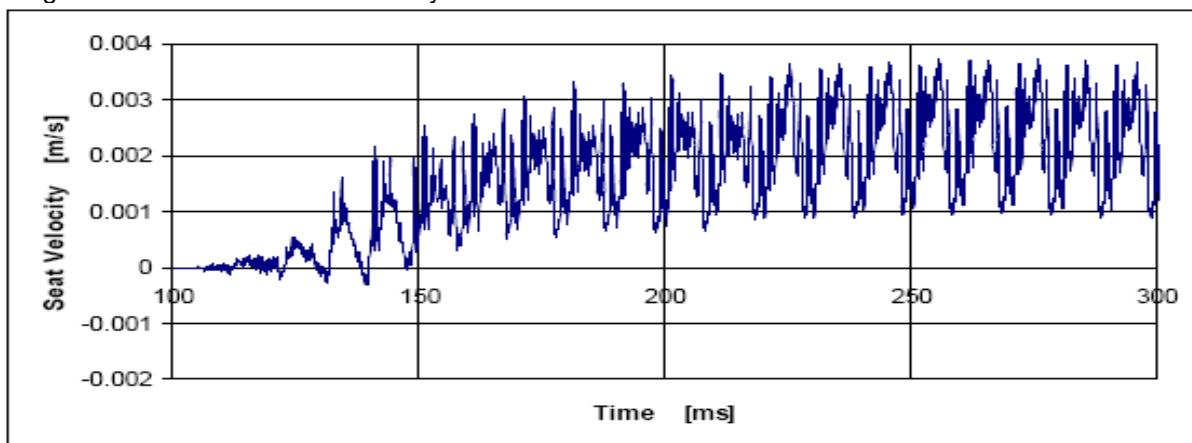


Figure 110: Seat Velocity-Time Chart for Machine #1 (YAMANASHI S) - Anti-personnel Mine

- Dynamic human body model

Analysis result (displacement) of the differential equation (1) is shown below:

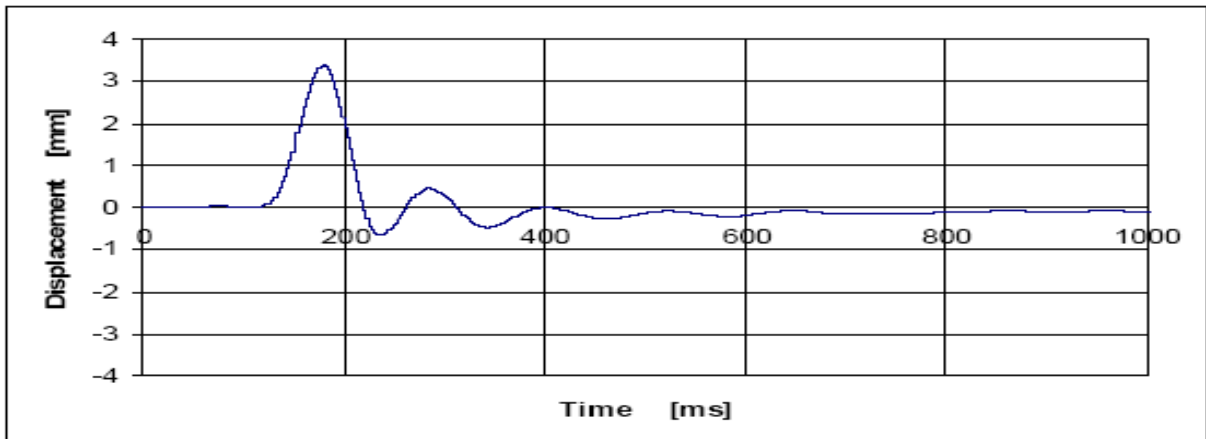


Figure 111: Simulated Human Body Displacement in Machine #1 (YAMANASHI S) - Anti-personnel Mine

- **ANTI-TANK MINE**

- Velocity-time chart

Integration of the seat acceleration by Anti – tank mine in section 11.2.4 is shown below:

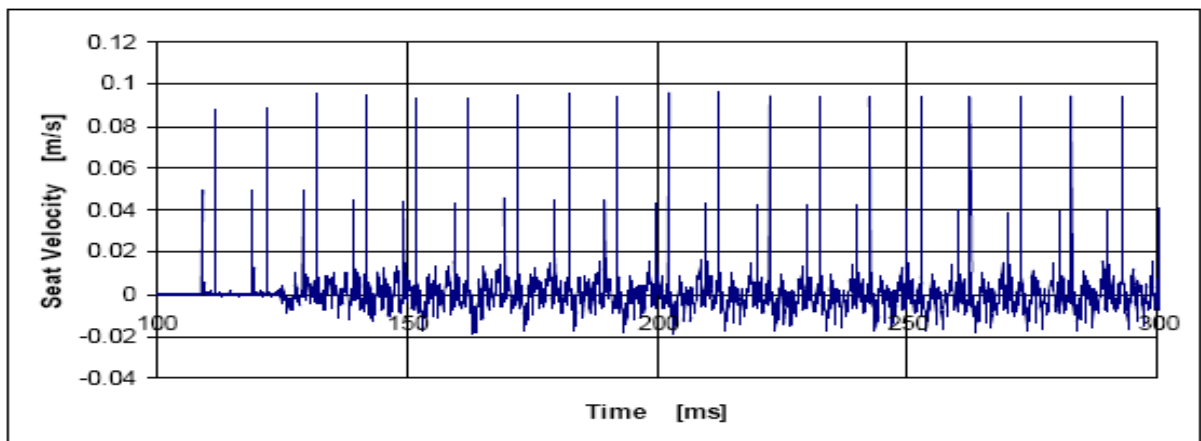


Figure 112: Seat Velocity-Time Chart for Machine #1 (YAMANASHI S) - Anti-tank Mine

- Dynamic human body model

An analysis result of the human body displacement derived from the differential equation (1) is shown in below.

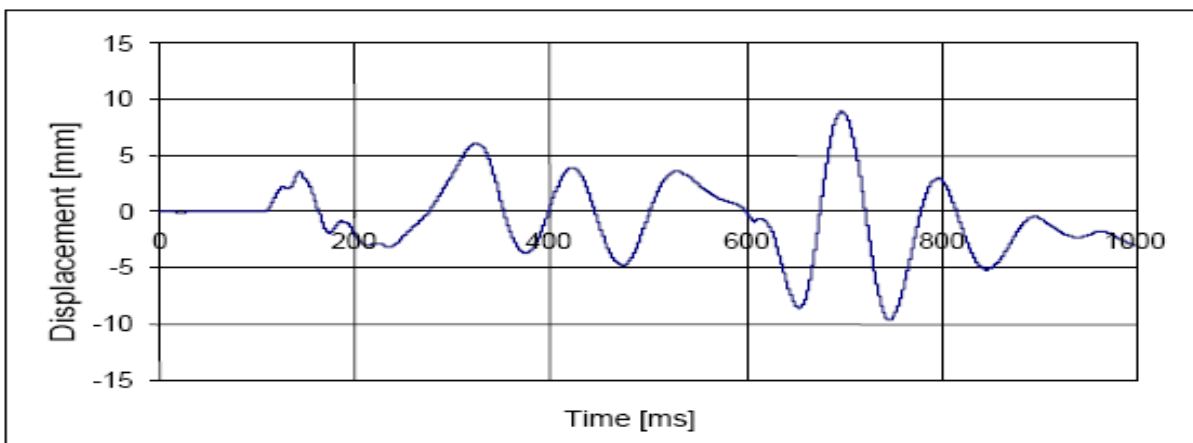


Figure 113: Machine #1 (Yamanashi S) Displacement of Human Body on the Operator Seat - Anti-Tank Mine